

Effects of double layer AlN buffer layers on properties of Si-doped Al_xGa_{1-x}N for improved performance of deep ultraviolet light emitting diodes

T. M. Al tahtamouni, J. Y. Lin, and H. X. Jiang

Citation: *J. Appl. Phys.* **113**, 123501 (2013); doi: 10.1063/1.4798239

View online: <http://dx.doi.org/10.1063/1.4798239>

View Table of Contents: <http://jap.aip.org/resource/1/JAPIAU/v113/i12>

Published by the [American Institute of Physics](#).

Related Articles

Influence of exciton lifetime on charge carrier dynamics in an organic heterostructure
[Appl. Phys. Lett.](#) **102**, 113304 (2013)

Influence of exciton lifetime on charge carrier dynamics in an organic heterostructure
[APL: Org. Electron. Photonics](#) **6**, 52 (2013)

Influence of internal absorption and interference on the optical efficiency of thin-film GaN-InGaN light-emitting diodes
[Appl. Phys. Lett.](#) **102**, 111111 (2013)

Metamorphic InAsSb/AlInAsSb heterostructures for optoelectronic applications
[Appl. Phys. Lett.](#) **102**, 111108 (2013)

Optical studies of the surface effects from the luminescence of single GaN/InGaN nanorod light emitting diodes fabricated on a wafer scale
[Appl. Phys. Lett.](#) **102**, 111906 (2013)

Additional information on J. Appl. Phys.

Journal Homepage: <http://jap.aip.org/>

Journal Information: http://jap.aip.org/about/about_the_journal

Top downloads: http://jap.aip.org/features/most_downloaded

Information for Authors: <http://jap.aip.org/authors>

ADVERTISEMENT



AIP Advances

Now Indexed in Thomson Reuters Databases

Explore AIP's open access journal:

- Rapid publication
- Article-level metrics
- Post-publication rating and commenting

Effects of double layer AlN buffer layers on properties of Si-doped $\text{Al}_x\text{Ga}_{1-x}\text{N}$ for improved performance of deep ultraviolet light emitting diodes

T. M. Al tahtamouni,^{1,a)} J. Y. Lin,² and H. X. Jiang²

¹*Department of Physics, Yarmouk University, Irbid 21163, Jordan*

²*Department of Electrical and Computer Engineering, Texas Tech University, Lubbock, Texas 79409, USA*

(Received 13 February 2013; accepted 8 March 2013; published online 22 March 2013)

Si-doped $\text{Al}_{0.77}\text{Ga}_{0.23}\text{N}$ epilayers were grown on AlN/sapphire templates by metal organic chemical vapor deposition using double AlN buffer layers. It was found that the use of double AlN buffer layers improved the overall material quality of the Si-doped $\text{Al}_{0.77}\text{Ga}_{0.23}\text{N}$ epilayers, as evidenced in the decreased density of screw dislocations and surface pits and increased emission intensity ratio of the band-edge to the deep level impurity transition. Hall effect measurements also indicated improved n-type conductivity. The performance of the deep ultraviolet light-emitting diodes fabricated using double buffer layers was significantly improved, as manifested by enhanced output power and reduced turn-on voltage. © 2013 American Institute of Physics. [<http://dx.doi.org/10.1063/1.4798239>]

Deep ultraviolet (DUV) light emitting diodes (LEDs) with emission wavelengths in the range of 200–340 nm have a wide range of potential applications, including environmental protection, bio-medicine, water purification, and high-density data storage.^{1,2} AlGa_N alloys have direct band gaps between 3.4 and 6.2 eV and are the prime choice for the realization of DUV LEDs. Si-doped AlGa_N plays a key role in UV LED structures as it serves as n-contact layer of the device. Electrons are injected from the n-contact through this layer into the active region. In order to maximize the carrier injection efficiency, the n-type AlGa_N layer needs to enable low contact resistance. Moreover, as the layer immediately below the active region, the n-type AlGa_N layer also serves as the template for the growth of the subsequent active region. The defect density in the active region will be strongly determined by the defect density in the n-type AlGa_N layer. Moreover, because the light output of the AlGa_N devices is generally extracted through the n-AlGa_N/sapphire side, the n-type AlGa_N layer also serves as a window for light output. For these reasons, it is highly desirable to seek methods and techniques to obtain n-type AlGa_N layers with high conductivity, high crystal quality, and high UV transparency. In particular, both highly conductive n-type and p-type AlGa_N alloys with high Al fraction are indispensable to obtain high performance DUV LEDs. However, highly conductive n-type Al-rich AlGa_N alloys are very difficult to achieve due in part to the generation of cation vacancy ($\text{V}_{\text{III}}^{3-}$) and cation vacancy complexes ($\text{V}_{\text{III}}\text{-complex}^{2-}$) during the growth.^{3–14} Dislocations may also introduce acceptor-like centers through dangling bonds along the dislocation line.¹⁵ Therefore, different methods have been employed to improve the conductivity of n-type AlGa_N epilayers, including indium–silicon codoping,^{16,17} using indium as a surfactant.¹⁸

In this letter, we report on the growth of Si-doped $\text{Al}_{0.77}\text{Ga}_{0.23}\text{N}$ epilayers on sapphire substrate using a double AlN buffer growth method and the incorporation of these Si-

doped layers into the DUV LEDs ($\lambda = 279$ nm) as n-type layers. Variable temperature Hall-effect (standard Van der Pauw) measurement was employed to study the electrical properties. X-ray diffraction (XRD) was used to determine the Al content as well as the crystalline quality of the epilayers. Atomic force microscopy (AFM) was used to probe the surface morphology. No cracks were found on the samples as revealed by AFM images. Photoluminescence (PL) spectroscopy was employed to investigate the optical properties of Si-doped $\text{Al}_{0.77}\text{Ga}_{0.23}\text{N}$ epilayers. The electroluminescence (EL) spectra and I–V characteristics of fabricated LEDs were also measured and discussed. By using a double AlN buffer growth method for the growth of the n-type AlGa_N layer, it was found that the overall quality, including the crystalline quality, surface morphology, PL intensity, and conductivity of the n-type AlGa_N epilayers exhibited remarkable improvements compared to n-type AlGa_N epilayers grown using a single AlN buffer growth method. The DUV LEDs fabricated with n-type AlGa_N epilayers grown using a double AlN buffer growth method exhibited improved performance.

Si-doped $\text{Al}_{0.77}\text{Ga}_{0.23}\text{N}$ epilayers of thickness 1.5 μm were grown on AlN/sapphire templates by metalorganic chemical vapor deposition (MOCVD). An AlN epilayer with a thickness of about 1.0 μm was first grown on sapphire (0001) substrate and followed by the growth of a Si-doped $\text{Al}_{0.77}\text{Ga}_{0.23}\text{N}$ epilayers. The targeted Si doping concentration was around $3 \times 10^{19} \text{ cm}^{-3}$ in all samples. The metalorganic sources used were trimethylaluminum and trimethylgallium for Al and Ga, respectively. Blue ammonia and silane (SiH_4) were used as nitrogen and silicon sources, respectively. The double AlN buffer growth method was initiated by a 15 nm low temperature (950 °C) AlN buffer layer (buffer 1) grown at 50 mbar followed by a second 100 nm AlN buffer layer (buffer 2) at 1100 °C grown at 50 mbar, and a 1.0 μm thick high temperature (1350 °C) AlN layer grown at 30 mbar,^{19,20} finally a 1.5 μm Si-doped $\text{Al}_{0.77}\text{Ga}_{0.23}\text{N}$ epilayer grown at 1050 °C and 50 mbar. Figure 1 shows the layer structures of

^{a)}Electronic mail: talal@yu.edu.jo.

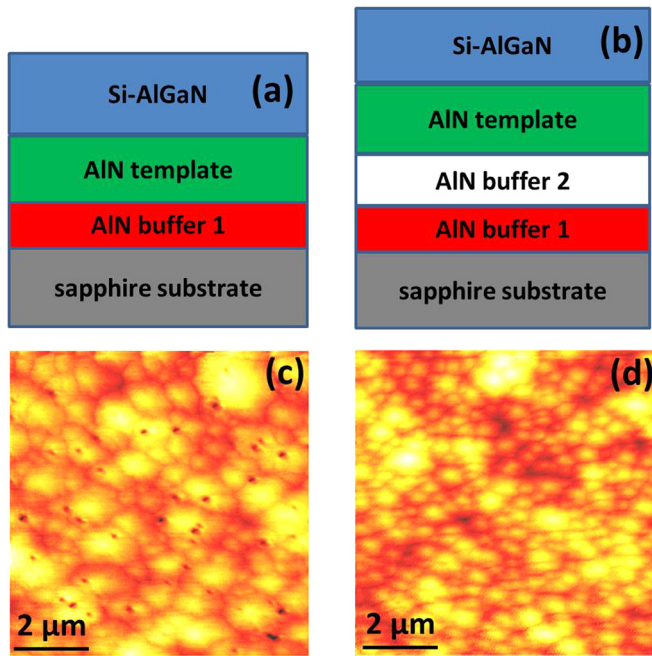


FIG. 1. (a) layer structure and (c) AFM image of a Si-doped $\text{Al}_{0.77}\text{Ga}_{0.23}\text{N}$ epilayer grown using single AlN buffer and (b) layer structure and (d) AFM image of a Si-doped $\text{Al}_{0.77}\text{Ga}_{0.23}\text{N}$ epilayer grown using double AlN buffer layers.

Si-doped $\text{Al}_{0.77}\text{Ga}_{0.23}\text{N}$ epilayers grown using (a) a single AlN buffer and (b) a double AlN buffer approach.

The total efficiency of DUV LEDs is substantially limited by the quality of the n-type AlGaIn layer grown before the active region. Threading dislocations (TDs) in the n-type AlGaIn layer continue to propagate into the active layers. These dislocations facilitate non-radiative recombination by providing allowed states within the bandgap. Consequently, we require the n-type AlGaIn layer to have a low TD density. Surface morphologies of both Si-doped $\text{Al}_{0.77}\text{Ga}_{0.23}\text{N}$ epilayers were studied by AFM. Figures 1(c) and 1(d) show, respectively, the AFM images of Si-doped $\text{Al}_{0.77}\text{Ga}_{0.23}\text{N}$ epilayers grown with single and double AlN buffer layers.

Root-mean-square (RMS) roughness is 2.3 nm and 1.5 nm, respectively, probed in a scanned area of $10 \times 10 \mu\text{m}^2$. The surface of Si-doped $\text{Al}_{0.77}\text{Ga}_{0.23}\text{N}$ epilayer grown using single AlN buffer in Fig. 1(c) is characterized by a larger density of surface pits (defects). The higher pits density reflects a higher TD density in the material.^{21,22} It is critical to reduce TD density in order to achieve high internal quantum efficiency. The surface of Si-doped $\text{Al}_{0.77}\text{Ga}_{0.23}\text{N}$ epilayer grown using double AlN buffer layers shown in Fig. 1(d) is almost clean. This indicates that double AlN buffer layers effectively decrease TD density by working as a dislocation filter.

XRD measurements were performed to determine the Al contents and crystalline quality of the Si-doped AlGaIn epilayers. Figure 2(a) shows the (002) ω - 2θ scan curves of the two Si-doped $\text{Al}_x\text{Ga}_{1-x}\text{N}$ epilayers grown using double (above) and single (below) AlN buffer layers. Taking the diffraction peak of AlN template at 36.02° as a reference point, the corresponding peaks of Si-doped $\text{Al}_x\text{Ga}_{1-x}\text{N}$ epilayers reveal almost the same position at 35.7° . The positions of the XRD peaks suggest that the molar fraction x in Si-doped $\text{Al}_x\text{Ga}_{1-x}\text{N}$ epilayers is around 0.77 in both samples. XRD rocking curves of the symmetric (002) reflection peak of Si-doped $\text{Al}_{0.77}\text{Ga}_{0.23}\text{N}$ epilayers are shown in Fig. 2(b). A full width at half maximum (FWHM) of 230 arc sec was obtained for the sample grown using double AlN buffer layers in comparison with 310 arc sec for the sample grown using single AlN buffer layer. The screw dislocation density can be estimated from the FWHM of the (002) XRD peak²³ and was seen to reduce from $\sim 2.0 \times 10^8$ in the sample with a single buffer layer to $1.13 \times 10^8 \text{ cm}^{-2}$ in the sample with double AlN buffer layers.

The room temperature (300 K) PL emission properties of Si-doped $\text{Al}_{0.77}\text{Ga}_{0.23}\text{N}$ epilayers have been investigated and the 300 K PL spectra are displayed in Fig. 3. In both samples, the band-edge emission line at around 5.34 eV is attributed to the localized exciton recombination (Refs. 24 and 25), whereas a stronger emission line around 2.98 eV is also evident. The origin of the deep level impurity transition

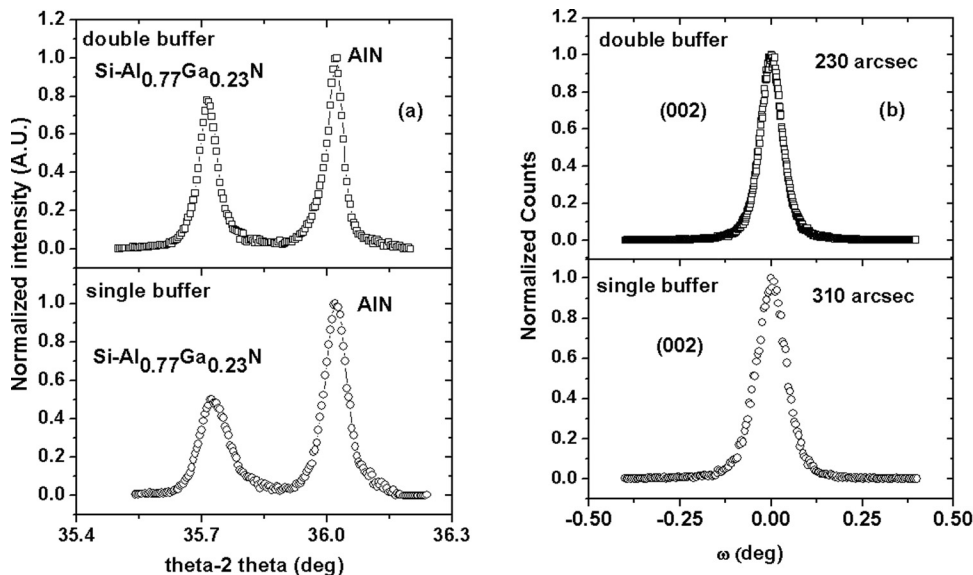


FIG. 2. (a) (002) ω - 2θ scans of the two Si-doped $\text{Al}_{0.77}\text{Ga}_{0.23}\text{N}$ epilayers grown using methods of a double AlN buffer (above) and single AlN buffer (below). (b) Rocking curves of the symmetric (002) reflection peaks in Si-doped $\text{Al}_{0.77}\text{Ga}_{0.23}\text{N}$ epilayers grown using double AlN buffer (above) and single AlN buffer (below).

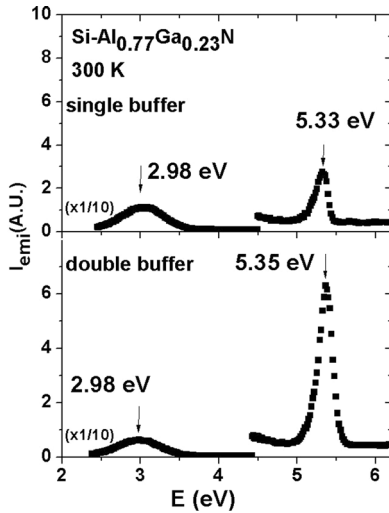


FIG. 3. Room temperature (300 K) photoluminescence spectra of a Si-doped $\text{Al}_{0.77}\text{Ga}_{0.23}\text{N}$ epilayer grown using a single AlN buffer and double AlN buffer.

at 2.98 eV has been well understood and is due to the recombination between shallow donors and cation vacancy complexes with two-negative charge ($\text{V}_{\text{III}} - \text{complex}$)²⁻⁴. The results shown in Fig. 3 clearly indicate that the intensity ratio of the band-edge emission (~ 5.34 eV) to the deep level impurity transition (~ 2.98 eV) increased by a factor of about 3 for the sample grown using double buffer layers. This is a direct consequence of an improved crystalline quality and a reduced TD density by employing the double buffer technique.

Figure 4(a) shows the I-V characteristics of as deposited Si-doped $\text{Al}_{0.77}\text{Ga}_{0.23}\text{N}$ epilayers with single and double AlN buffers. It is apparent that Si-doped $\text{Al}_{0.77}\text{Ga}_{0.23}\text{N}$ epilayer with double buffer layers exhibits a lower resistance compared to the Si-doped $\text{Al}_{0.77}\text{Ga}_{0.23}\text{N}$ epilayer with single AlN buffer. Figure 4(b) shows the variation of resistivity of both Si-doped $\text{Al}_{0.77}\text{Ga}_{0.23}\text{N}$ epilayers with temperature in the range between 245 and 345 K. The resistivity decreases exponentially with

increasing temperature for both samples. At room temperature, the resistivity of Si-doped $\text{Al}_{0.77}\text{Ga}_{0.23}\text{N}$ epilayer grown using double AlN buffer layers is $0.033 \Omega \text{ cm}$, while the resistivity of Si-doped $\text{Al}_{0.77}\text{Ga}_{0.23}\text{N}$ epilayer grown using single AlN buffer is $0.045 \Omega \text{ cm}$. The improved electrical conductivity in Si-doped $\text{Al}_{0.77}\text{Ga}_{0.23}\text{N}$ epilayer grown using double AlN buffer layers is directly related to the reduction of cation vacancies and their complexes. The reduction in resistivity of Si-doped AlGaN is a critical step to achieve DUV emitters with an enhanced current injection efficiency.

The Si-doped $\text{Al}_{0.77}\text{Ga}_{0.23}\text{N}$ epilayers have been incorporated into the DUV LED ($\lambda = 279 \text{ nm}$) structures as n-type layers. Two DUV LEDs were grown, one using double AlN buffers and the other using single AlN buffer on AlN/sapphire substrates. A high-quality undoped AlN epilayer was first grown on (0001) sapphire as a template. A Si-doped $\text{Al}_{0.77}\text{Ga}_{0.23}\text{N}$ layer of thickness $1.5 \mu\text{m}$ was then grown on this AlN/sapphire template, followed by a 5-layer MQW consisting of 1.5 nm thick $\text{Al}_{0.50}\text{Ga}_{0.50}\text{N}$ wells and 6 nm thick $\text{Al}_{0.70}\text{Ga}_{0.30}\text{N}$ barriers and a 10 nm Mg-doped $\text{Al}_{0.75}\text{Ga}_{0.25}\text{N}$ electron blocking layer. The structure was then completed with a 30 nm thick p- $\text{Al}_{0.20}\text{Ga}_{0.90}\text{N}$ and a 100 nm thick p-GaN contact layer. The targeted Mg doping concentration was around $2 \times 10^{20} \text{ cm}^{-3}$ in both p- $\text{Al}_{0.20}\text{Ga}_{0.90}\text{N}$ and p-GaN layers. DUV LEDs were fabricated with a circular geometry and the device fabrication procedure has been described elsewhere.²⁶

Figure 5 shows the I-V characteristics (a), and the EL spectra (b) of the two DUV LEDs with a $300 \mu\text{m}$ diameter size. The EL spectra were measured at a forward current of 40 mA . It can be seen in Fig. 5(a) that the use of double AlN buffer layers reduces both the serial resistance and the turn-on voltage of the DUV LED. The turn-on voltage, V_f , of DUV LEDs with double and single AlN buffers are 5.2 V and 6.7 V , respectively. Improvements in both the emission intensity and the width of the EL spectra are also evident in Fig. 5(b). The EL intensity of DUV LED with double AlN buffer layers is 1.5 times stronger than that of DUV LED

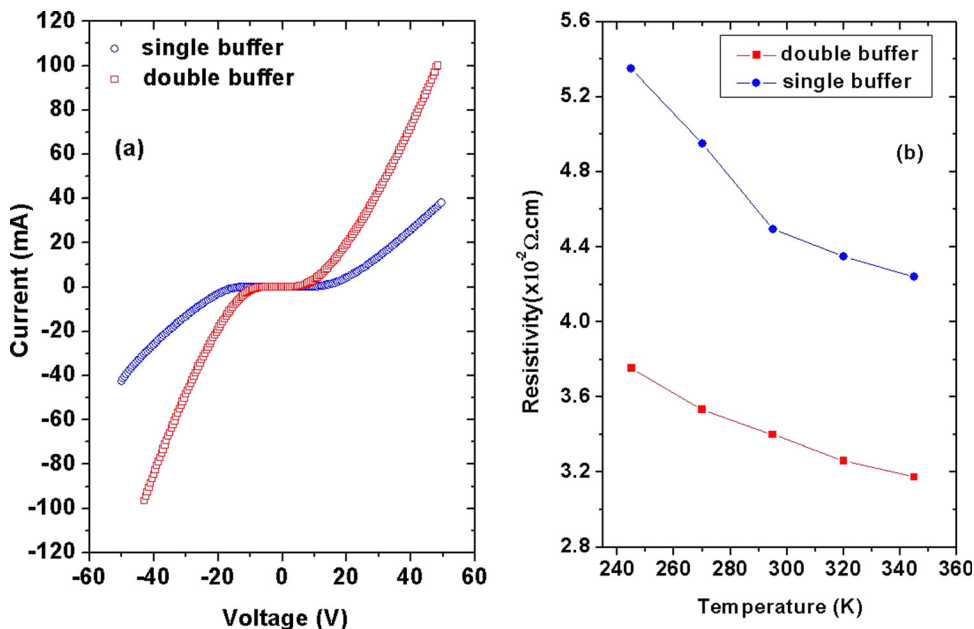


FIG. 4. (a) Current-voltage ($I-V$) curves for as deposited Si-doped $\text{Al}_{0.77}\text{Ga}_{0.23}\text{N}$ with single and double AlN buffer. (b) Temperature variation of resistivity of Si-doped $\text{Al}_{0.77}\text{Ga}_{0.23}\text{N}$ with single and double AlN buffer in the temperature range of 245–345 K.

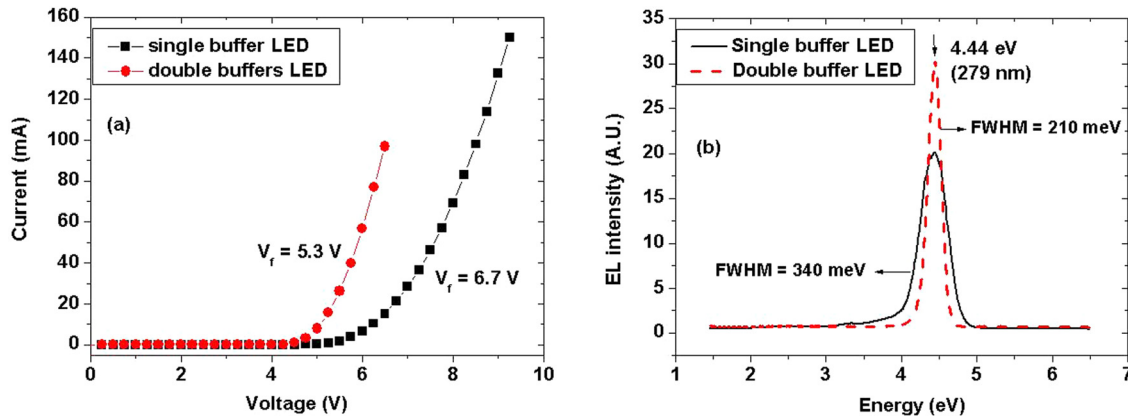


FIG. 5. (a) Current-voltage (I - V) characteristics and (b) EL properties for DUV LED devices incorporating Si-doped $\text{Al}_{0.77}\text{Ga}_{0.23}\text{N}$ with single and double AlN buffer.

with single AlN buffer. The full width at half maximum (FWHM) of EL spectra of DUV LEDs with double and single AlN buffers are 210 meV (13 nm) and 340 eV (21 nm), respectively. The results shown in Fig. 5 are a direct consequence of the use of double AlN buffer layers that reduces TD density leading to a lower resistivity and better crystalline quality of the device structure, which we believe is a useful strategy to enhance the performance of DUV LEDs.

In summary, the use of double AlN buffer layer growth method was shown to reduce the density of threading dislocations, improve crystalline quality, and lower the resistivity of Si-doped $\text{Al}_{0.77}\text{Ga}_{0.23}\text{N}$ epilayers. Incorporating these Si-doped $\text{Al}_{0.77}\text{Ga}_{0.23}\text{N}$ epilayers as n-type layers into the DUV LED layer structures enhanced the output power and reduced the turn-on voltage of the DUV LEDs.

T. M. Al tahtamouni is grateful to the Deanship of Scientific Research and Graduate Studies at Yarmouk University for the support. H. X. Jiang and J. Y. Lin are grateful to the AT&T Foundation for the support of Ed Whitacre and Linda Whitacre Endowed chairs.

¹V. Adivarahan, Q. Fareed, S. Srivastava, T. Katona, M. Gaevski, and A. Khan, *Jpn. J. Appl. Phys., Part 2* **46**, L537 (2007).

²T. M. Al Tahtamouni, N. Nepal, J. Y. Lin, H. X. Jiang, and W. W. Chow, *Appl. Phys. Lett.* **89**, 131922 (2006).

³K. B. Nam, J. Li, M. L. Nakarmi, J. Y. Lin, and H. X. Jiang, *Appl. Phys. Lett.* **81**, 1038 (2002).

⁴N. Nepal, M. L. Nakarmi, J. Y. Lin, and H. X. Jiang, *Appl. Phys. Lett.* **89**, 092107 (2006).

⁵K. B. Nam, M. L. Nakarmi, J. Y. Lin, and H. X. Jiang, *Appl. Phys. Lett.* **86**, 222108 (2005).

⁶Y. Taniyasu, M. Kasu, and N. Kobayashi, *Appl. Phys. Lett.* **81**, 1255 (2002).

⁷M. L. Nakarmi, K. H. Kim, K. Zhu, J. Y. Lin, and H. X. Jiang, *Appl. Phys. Lett.* **85**, 3769 (2004).

⁸K. Zhu, M. L. Nakarmi, K. H. Kim, J. Y. Lin, and H. X. Jiang, *Appl. Phys. Lett.* **85**, 4669 (2004).

⁹Y. Taniyasu, M. Kasu, and T. Makimoto, *Appl. Phys. Lett.* **85**, 4672 (2004).

¹⁰M. L. Nakarmi, N. Nepal, J. Y. Lin, and H. X. Jiang, *Appl. Phys. Lett.* **86**, 261902 (2005).

¹¹J. Neugebauer and C. G. Van de Walle, *Appl. Phys. Lett.* **69**, 503 (1996).

¹²T. Mattila and R. M. Nieminen, *Phys. Rev. B* **55**, 9571 (1997).

¹³C. Stampfl and C. G. Van de Walle, *Phys. Rev. B* **65**, 155212 (2002).

¹⁴S. T. Bradley, S. H. Goss, L. J. Brillson, J. Hwang, and W. J. Schaff, *J. Vac. Sci. Technol. B* **21**, 2558 (2003).

¹⁵B. Podor, *Phys. Status Solidi* **16**, K167 (1966).

¹⁶P. Cantu, S. Keller, U. Mishra, and S. DenBaars, *Appl. Phys. Lett.* **82**, 3683 (2003).

¹⁷V. Adivarahan, G. Simin, G. Tamulaitis, R. Srinivasan, J. Yang, A. Khan, M. Shur, and R. Gaska, *Appl. Phys. Lett.* **79**, 1903 (2001).

¹⁸T. M. Al tahtamouni, A. Sedhain, J. Y. Lin, and H. X. Jiang, *Appl. Phys. Lett.* **92**, 092105 (2008).

¹⁹T. M. Al Tahtamouni, J. Li, J. Y. Lin, and H. X. Jiang, *J. Phys. D: Appl. Phys.* **45**, 285103 (2012).

²⁰T. M. Al tahtamouni, J. Y. Lin, and H. X. Jiang, *Appl. Phys. Lett.* **101**, 192106 (2012).

²¹P. Cantu, F. Wu, P. Waltereit, S. Keller, A. E. Romanov, U. K. Mishra, S. P. DenBaars, and J. S. Speck, *Appl. Phys. Lett.* **83**, 674 (2003).

²²X. H. Wu, P. Fini, E. J. Tarsa, B. Heying, S. Keller, U. K. Mishra, S. P. DenBaars, and J. S. Speck, *J. Cryst. Growth* **189/190**, 231 (1998).

²³B. N. Pantha, R. Dahal, M. L. Nakarmi, N. Nepal, J. Li, J. Y. Lin, and H. X. Jiang, *Appl. Phys. Lett.* **90**, 241101 (2007).

²⁴H. S. Kim, R. A. Mair, J. Li, J. Y. Lin, and H. X. Jiang, *Appl. Phys. Lett.* **76**, 1252 (2000).

²⁵G. Coli, K. K. Bajaj, J. Li, J. Y. Lin, and H. X. Jiang, *Appl. Phys. Lett.* **80**, 2907 (2002).

²⁶K. H. Kim, Z. Y. Fan, M. Khizar, M. L. Nakarmi, J. Y. Lin, and H. X. Jiang, *Appl. Phys. Lett.* **85**, 4777 (2004).